A Journal of the Gesellschaft Deutscher Chemiker

Angewandte International Edition GDCh Chemie

www.angewandte.org

Accepted Article

Title: A bipolar and self-polymerized phthalocyanine complex for fast and tunable energy storage

Authors: Shuyan Song, Hengguo Wang, Lanlan Wu, Yu Liu, Haidong Wang, Zhenjun Si, Qiang Li, Qiong Wu, Qi Shao, Yinghui Wang, and Hongjie Zhang

To be cited as: *Angew. Chem. Int. Ed.* 10.1002/anie.201904242
Angew. Chem. 10.1002/ange.201904242

Link to VoR: http://dx.doi.org/10.1002/anie.201904242
http://dx.doi.org/10.1002/ange.201904242

WILEY-VCH

10.1002/anie.201904242

WILEY-VCH

A bipolar and self-polymerized phthalocyanine complex for fast and tunable energy storage

Heng-guo Wang,[a,b] Haidong Wang,[b] Zhenjun Si,[b] Qiang Li,[b] Qiong Wu,[b] Qi Shao,[b] Lanlan Wu,[a] Yu Liu,[a] Yinghui Wang,[a] Shuyan Song*[a] and Hongjie Zhang[a]

Abstract: Bipolar redox organics have attracted immense scientific interest as electrode materials for energy storage due to their flexibility, sustainability and environmental friendliness. However, an understanding of their application in all-organic batteries, let alone dual-ion batteries (DIBs), is in its infancy and demands prompt attention. Herein, we propose a molecular-level design strategy to screen a variety of phthalocyanine-based bipolar organics. Based on the bipolar and self-polymerized features, the resulting Cu tetraaminephthalocyanine (CuTAPc) shows multifunctional applications in various energy storage systems, including lithium-based DIBs using CuTAPc as the cathode material, graphite-based DIBs using CuTAPc as the anode material and symmetric DIBs using CuTAPc as both the cathode and anode materials. Notably, in lithium-based DIBs, the use of CuTAPc as the cathode material results in a high discharge capacity of 236 mAh g^{-1} at 50 mA g^{-1} and a high reversible capacity of 74.3 mAh g^{-1} after 4000 cycles at 4 A g^{-1}. Most importantly, a high energy density of 239 Wh kg^{-1} and power density of 11.5 kW kg^{-1} can be obtained in all-organic symmetric DIBs.

Organic compounds are famous for their structural diversity, which can be tailored by simply adding, removing, or substituting functional groups.[1] In fact, even a simple functional group has its own function that affects the properties of organic compounds, which endows them with design flexibility for various applications.[2] Undoubtedly, this structural diversity is necessary to optimize organic compounds as electrode materials for electrochemical energy-storage systems (EESs).[3] For example, the incorporation of electron-withdrawing/donating groups could elevate/reduce the redox potentials,[4] or the formation of polymers could suppress the dissolution of small molecule compounds.[5] In addition, organic compounds are available in natural resources or can be synthesized by relatively moderate synthetic routes, thus showing environmentally friendly features and minimal environmental footprints.[6] From the perspective of sustainability, organic electrode materials are promising alternatives to conventional transitional metal-based electrode materials that are mined from minerals or synthesized using high temperature.

To date, various types of organic electrode materials based on the different redox reactions, including n-, p-, or bipolar-type, have attracted widespread interest for EESs.[7] For n-type organics, the neutral state first accepts electrons to form a negatively charged state, and then cations (Li^+, Na^+, K^+ or even H^+) can be used to neutralize the negative charge. Whereas for p-type organics, electrons can first be extracted to form a positively charged state, then anions (PF_6^-, ClO_4^-, BF_4^- or $TFSI^-$) can be used to neutralize the positively charged state. By contrast, bipolar-type organics could utilize negatively or positively charged states to interact with the cations or anions mentioned above, which extends their applications to lithium ion batteries (LIBs), electrochemical capacitors, and even dual-ion batteries.

Porphyrin and phthalocyanine, typically planar aromatic macrocyclic molecule, show bipolar features of donating or accepting electrons, and their 18 π-electrons can be oxidized or reduced into 16 π-electrons or 20 π-electrons, respectively.[8] Moreover, their small HOMO-LUMO gaps can assist in the facile injection and removal of electrons, resulting in fast redox kinetics.[9] In addition, the highly stable C-N bonds in their frameworks can endow them with a high reversible capacity and large working voltage.[7c] In this context, the development of porphyrin/phthalocyanine-based derivatives or polymers as electrode materials for EESs has been reported.[10] However, there are still several limitations on their synthesis and electrochemical performance. For example, simplifying the synthetic method needs to be addressed for their practical application. Furthermore, the relatively high molecular weight resulting from the inactive linking groups reduces the capacity of porphyrin-based polymers.

To overcome these issues, we demonstrate that metallophthalocyanine derivatives can be successfully served as electrode materials for EESs. Herein, a molecular-level design strategy is presented to screen high-performance and easily synthesized phthalocyanine-based electrode materials. As a result, the Cu tetraaminephthalocyanine (CuTAPc) possesses bipolar and self-polymerized features. Interestingly, polymeric phthalocyanine can be formed by the electropolymerization of CuTAPc without the need for additional linking groups, resulting in high capacity and improved cycling stability. Most importantly, the bipolar feature endows CuTAPc with multifunctional applications, including lithium-based and graphite-based dual ion batteries (LDIBs and GDIBs), and symmetric dual ion batteries (SDIBs). To the best of our knowledge, there are scarce reports on bipolar redox organics as high-performance electrode-active material in DIBs, let alone all-organic symmetric DIBs.

Phthalocyanines are centrosymmetric planar 18 π-electron aromatic macrocycles with four nitrogen-linked isoindole units that have a central cavity that can bind various metal ions to form metal phthalocyanines.[8] As a proof-of-concept demonstration, the structure of CuTAPc as well as its two-electron oxidation (+2 charge state) and two-electron reduction (-2 charge state) are shown in Figure 1a. Notably, 18 π-electron phthalocyanine can be oxidized into dicationic species (+2

[a] Dr. H. Wang, Dr. L. Wu, Y. Liu, Dr. Y. Wang, Prof. S. Song and Prof. H. Zhang
State Key Laboratory of Rare Earth Resource Utilization, Changchun Institute of Applied Chemistry, Chinese Academy of Sciences, Changchun 130022, Jilin (China)
E-mail: songsy@ciac.ac.cn
[b] Dr. H. Wang, H. Wang, Prof. Dr. Z. Si, Q. Li, Q. Wu and Q. Shao, School of Materials Science and Engineering, Changchun University of Science and Technology, Changchun 130022, Jilin (China)

Supporting information for this article is given via a link at the end of the document.

charge state, 16 π-electrons) or reduced into dianionic species (-2 charge state, 20 π-electrons), respectively.[10a,10c] To investigate the oxidation/reduction process of CuTAPc, density functional theory (DFT) is used to calculate the HOMO/LUMO energy levels (Figure S1). Clearly, CuTAPc has a very low LUMO energy level that endows it with good oxidizability and a high reduction potential and a small LUMO-HOMO gap that endows it with good electronic conductivity and fast redox kinetics.[4f,5d] These features enable CuTAPc to be a bipolar-type electrode material, which can utilize its negatively or positively charged states to interact with cations (Li^+, Na^+, K^+ or H^+) or anions (PF_6^-, ClO_4^-, BF_4^- or $TFSI^-$), respectively. Encouraged by its redox mechanism, different polarity-switchable cells are designed and constructed (Figure 1b). Coupled with a counter electrode (Li foil), CuTAPc can be used as a cathode material in LDIBs (cell 1) or an anode material in LIBs (cell 2). Interestingly, coupled with graphite or itself, CuTAPc could be assembled into GDIBs (cell 3) or SDIBs (cell 4).

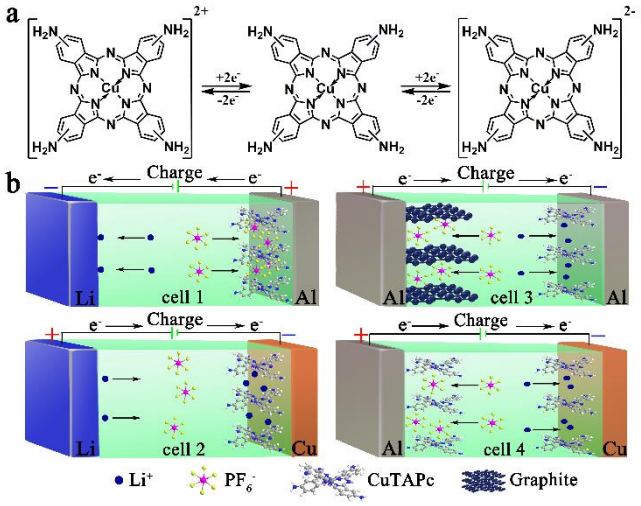

Figure 1. (a) Two-electron oxidation (+2 charge state) and two-electron reduction (-2 charge state) of CuTAPc. (b) Various cell configurations for using CuTAPc as a bipolar electrode material.

To screen high-performance phthalocyanine-based electrode materials, we design and synthesize two categories of phthalocyanine derivatives with different central metal ions, such as none, Cu, Fe, or Co, and different substitutional groups, such as none, $-NO_2$, $-NH_2$, -OH, or -N=C-Ph (Figure 2a, detailed synthesis and characterization of these compounds are shown in Supporting Information and Figure S2). To compare the effects of the different functional groups, their electrochemical performance in cell 1 is investigated. By contrast, CuTAPc shows the optimal cycling performance (Figure S3), which could be attributed to the strong interaction between CuTAPc and PF_6^- (Figure 2b) and the electropolymerization of the CuTAPc monomers (Figure S4). On one hand, the high binding energy of -4.72 eV suggests the stronger affinity of CuTAPc toward PF_6^- (Figure S5). On the other hand, this transformation from monomeric CuTAPc to polymeric CuTAPc could be preliminary verified by *ex situ* FTIR analysis (Figure S6). To further confirm this transformation, the electropolymerization of CuTAPc is performed using a three-electrode system (detailed methods for the electropolymerization process are shown in Supporting Information).[11] An irreversible oxidation peak at approximately 0.35 V is observed in the CV curves of CuTAPc, which weakens and disappears during cycling (Figures S7); however, other phthalocyanine derivatives show reversible redox peaks during the first and subsequent cycles (Figures S8), indicating the oxidative electropolymerization of CuTAPc. In addition, *ex situ* FTIR can confirm the formation of polymeric CuTAPc due to the absence of the characteristic peaks for $-NH_2$ (Figure S9). Intuitively, the glassy carbon electrode is coated by a blue-black film that is visible to the naked eye after cycling only for CuTAPc (Figure S10), which confirms the formation of the polymer. In addition, DFT is also used to calculate the HOMO/LUMO energy levels of CuTAPc dimer (Figure 2c). Compared with the CuTAPc monomer, the CuTAPc dimer shows a decrease in the LUMO energy and an increase in the HOMO energy. The smaller LUMO-HOMO gap indicates increased electronic conduction,[9] indicating that CuTAPc could show enhanced electrical conductivity after the initial cycle.

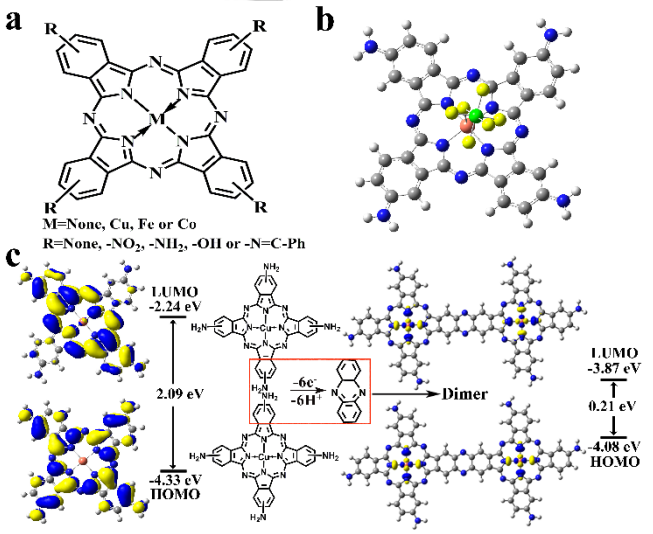

Figure 2. (a) Molecular structure of the various phthalocyanine derivatives. (b) Geometry of PF_6^- binding to CuTAPc. (c) Energy level diagrams of CuTAPc and its dimer obtained from DFT calculations.

The electrochemical properties of CuTAPc as the cathode material in cell 1 are investigated in detail. During the charge process, CuTAPc can be oxidized into a dicationic species ($CuTAPc^{2+}$, 16 π-electrons) that could capture PF_6^- from the electrode; at the same time, the Li^+ from the electrolyte could move to the anode. Conversely, during the discharge process, $CuTAPc^{2+}$ is reduced into electrically natural CuTAPc, or even the dianionic species ($CuTAPc^{2-}$, 20 π-electrons), and then PF_6^- dissolve back into the electrolyte to react with the Li^+ released from the anode to form stable $LiPF_6$.[7c,12] This hypothesis can be verified by *ex situ* FTIR, element mapping and XPS analysis (Figure S11-S13). To confirm the redox reaction, cyclic voltammograms (CVs) are obtained (Figure 3a). During the first anodic scan, an obvious irreversible oxidative peak can be observed at 3.6 V. After the first anodic scan, the highly reversible CV curves remain. These results are in accordance with the irreversible feature observed in the three-electrode

10.1002/anie.201904242

system, which further confirms the self-polymerizing feature of CuTAPc. Furthermore, the charge/discharge curves and the corresponding dQ/dV curve also show similar features (Figure 3b and Figure S14a). In addition to the irreversible initial charge capacity, CuTAPc could deliver high charge/discharge capacities of 300 and 236 mAh g^{-1}, respectively, along with a Coulombic efficiency (CE) of 78.8% at 50 mA g^{-1}. Herein, carbon black shows the negligible capacity contribution (Figure S14b). Interestingly, the charge/discharge capacities of 112.9/112.3 mAh g^{-1} at 300 mA g^{-1} are retained after 200 cycles (Figure 3c). At a high current density of 4 A g^{-1}, CuTAPc also displays high initial charge/discharge capacities of 192.9/151.9 mAh g^{-1} and maintains high charge/discharge capacities of 74.3/75.4 mAh g^{-1} after 4000 cycles (Figure 3d). Even at a very high current density of 20 A g^{-1}, CuTAPc delivers a high reversible capacity of 109 mAh g^{-1} (Figure 3e). Moreover, after back and forth deep cycling over 300 cycles, a high reversible capacity of 155.4 mAh g^{-1} is recovered when the current density is returned to 1 A g^{-1}. Obviously, CuTAPc shows an excellent rate capability, which could be attributed to the reduced charge-transfer resistance (Figure S15). To further reveal the reasons for the high-rate capability, a detailed kinetic analysis was conducted by CV curves at various scan rates (Figure 3f).[13] Based on the equation $i = av^b$, the b values, an indicator of the electrochemical behavior, are determined to be 0.997 and 0.996 (Figure 3g). Herein, the b value approaches 1.0, indicating a capacitive mechanism of PF_6^- storage for CuTAPc. The capacitive contribution can be quantitatively determined; for example, CuTAPc shows 92.57% of the capacitance contribution at a scan rate of 0.6 mV s^{-1} (Figure S16). The capacitive contribution increases from 84.43% to 99.23% as the scan rate increases from 0.2 to 1.0 mV s^{-1} (Figure 2h), indicating a capacitive mechanism, especially at high rates.

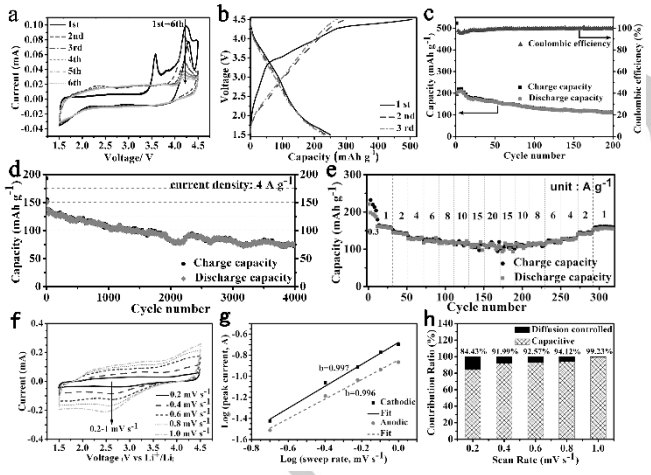

Figure 3. Electrochemical performance of CuTAPc as the cathode material in cell 1. (a) CV curves in the range of 4.5-1.5 V at 0.1 mV s^{-1}. (b) Charge-discharge curves at 50 mA g^{-1} and cycling performance at 0.3 A g^{-1} (c) and 4 A g^{-1} (d). (e) Rate performance at various current densities. (f) CV curves at different scan rates. (g) the corresponding plots log(*i*) versus log(*v*) at each redox peak and (h) contribution ratio of the pseudocapacitance at various scan rates.

To confirm the bipolar feature, CuTAPc is used as the anode material to construct conventional LIBs (cell 2), which could show good Li^+ storage properties (Figures S17-S21). Furthermore, coupled with graphite, CuTAPc could be assembled into asymmetric GDIBs (cell 3), which also delivers good energy storage properties (Figure S22-S23). CV curves of GDIBs show three pairs of oxidation/reduction peaks, corresponding to the different interaction processes of PF_6^-/Li^+ into/out of the graphite/CuTAPc (Figure S24).[12a,14] In cell 3, CuTAPc as the anode material could experience both the reduced (n-doped) and oxidized (p-doped) state, that is, a transformation from $[CuTAPc]^{2-}$ to $[CuTAPc]^{2+}$, during which PF_6^- and Li^+ from the $LiPF_6$ electrolyte could insert/deinsert graphite and CuTAPc, respectively (for details, see the Supporting Information). This hypothesis could be further confirmed by XRD patterns, element mapping and XPS analysis (Figure S25-S27).

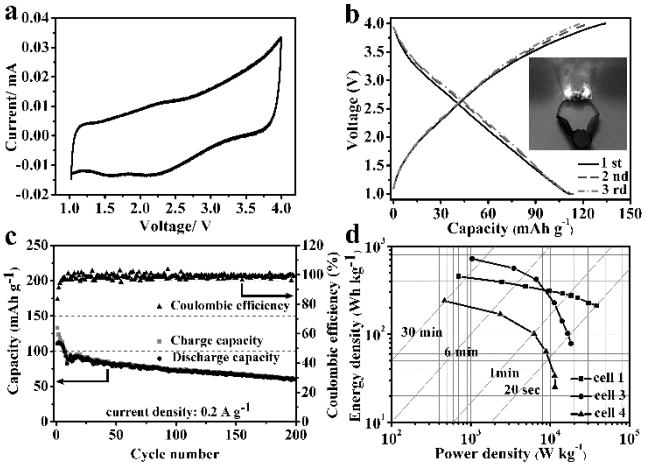

Figure 4. (a) CV curves of the SDIB in the range of 4.0-1.0 V at 0.1 mV s^{-1}. (b) Charge/discharge profiles of the SDIB (the inset shows that a coin full cell can light a small LED lamp). (c) Cycling performance of the SDIB at 0.2 A g^{-1}. (d) Ragone plots of cell 1, cell 3 and cell 4.

To completely demonstrate the bipolar feature of CuTAPc, a symmetric system using CuTAPc as both the cathode and anode materials was constructed. CV curves are first used to explore the fundamental electrochemical properties of the symmetric system (Figure 4a), which shows no well-defined voltage plateau, suggesting rapid multiple redox reactions from the oxidized (p-doped) and reduced (n-doped) state, that is, a transformation from $[CuTAPc]^{2+}$ to $[CuTAPc]^{2-}$ (for details, see the Supporting Information).[7c] The typical charge/discharge curves show a broad operating voltage window and a similar voltage profile as the CV curves (Figure 4b). Interestingly, the SDIBs can light two-series-connected LEDs (inset of Figure 4b). In addition, the SDIBs show initial charge/discharge capacities of 133.2/110.9 mAh g^{-1} at 0.2 A g^{-1} along with a CE of 83.2% and a high reversible capacity of 60.1 mAh g^{-1} after 200 cycles with a capacity retention of 54.2% (Figure 4c). Moreover, even at very high current density of 10 A g^{-1}, GDIBs delivers a high reversible capacity of 22.5 mAh g^{-1} (Figure S28), indicating the superior rate performance. Furthermore, cell 1 shows a high specific energy of 454 Wh kg^{-1} and a specific power of 38.4 kW kg^{-1}, cell 3 shows a high specific energy of 719.5 Wh kg^{-1} and a specific power of 18.3 kW kg^{-1}, while cell 4 shows a high specific energy of 239 Wh kg^{-1} and a specific power of 11.5 kW kg^{-1} (Figure 4e),

which can even compete with organic-based batteries[7c,10c,12b] and graphite-based dual ion batteries.[14a,14c]

In summary, for the first time, our findings confirm that CuTAPc exhibits bipolar and self-polymerized features, which can be used as the electrode materials for DIBs, including all-organic symmetric DIBs. Coupled with a lithium counter electrode, CuTAPc can be used as a high-performance cathode material or anode material; for example, as the cathode material, it presents a high initial capacity of 236 mAh g^{-1} at 50 mA g^{-1} and a high reversible capacity of 74.3 mAh g^{-1} after 4000 cycles at 4 A g^{-1}. More encouragingly, coupled with graphite or itself, CuTAPc could be assembled into asymmetric and symmetric full cells; for example, symmetric full cells could display a high specific energy of 239 Wh kg^{-1} and a specific power of 11.5 kW kg^{-1}, surpassing many state-of-art materials. We believe that this work can open up new pathways to construct organic-based energy storage systems.

Acknowledgements

The authors are grateful for the financial aid from the National Natural Science Foundation of China (Grant Nos. 21590794, 21771173, 21521092 and 51502284), K. C. Wong Education Foundation (GJTD-2018-09), the Science & Technology Department of Jilin Province (Grant No. 20170101177JC, 20170101186JC and 20180101179JC), and the CAS-CSIRO project (Grant No. GJHZ1730).

Keywords: phthalocyanine derivatives • self-polymerization• bipolar organics • all-organic symmetric batteries • dual ion batteries

[1] a) M. Armand, J. M. Tarascon, *Nature* **2008**, *451*, 652-657; b) M. Lee, J. Hong, J. Lopez, Y. Sun, D. Feng, K. Lim, W. C. Chueh, M. F. Toney, Y. Cui, Z. Bao, *Nat. Energy* **2017**, *2*, 861-868; c) G. Milczarek, O. Inganas, *Science* **2012**, *335*, 1468-1471; d) S. Muench, A. Wild, C. Friebe, B. Häupler, T. Janoschka, U. S. Schubert, *Chem. Rev.* **2016**, *116*, 9438-9484; e) X. M. Hu, M. H. Rønne, S. U. Pedersen, T. Skrydstrup, K. Daasbjerg, *Angew. Chem. Int. Ed.* **2017**, *56*, 6468-6472.

[2] a) W. Zhang, W. Lai, R. Cao, *Chem. Rev.* **2017**, *117*, 3717-3797; b) H. Lu, N. Kobayashi, *Chem. Rev.* **2016**, *116*, 6184-6261; c) Y. Lin, W. J. Feng, J. J. Zhang, Z. H. Xue, T. J. Zhao, H. Su, S. I. Hirano, X. H. Li, J. S. Chen, *Angew. Chem. Int. Ed.* **2018**, *57*, 12563-12566; d) P. T. Smith, B. P. Benke, Z. Cao, Y. Kim, E. M. Nichols, K. Kim, C. J. Chang, *Angew. Chem. Int. Ed.* **2018**, *57*, 9684-9688; e) C. Luo, X. Ji, J. Chen, K. J. Gaskell, X. He, Y. Liang, J. Jiang, C. Wang, *Angew. Chem. Int. Ed.* **2018**, *57*, 8567-8571.

[3] a) Z. Guo, Y. Ma, X. Dong, J. Huang, Y. Wang, Y. Xia, *Angew. Chem. Int. Ed.* **2018**, *57*, 11737-11741; b) Z. Luo, L. Liu, J. Ning, K. Lei, Y. Lu, F. Li, J. Chen, *Angew. Chem. Int. Ed.* **2018**, *57*, 9443–9446; c) C. Ma, X. Zhao, L. Kang, K. X. Wang, J. S. Chen, W. Zhang, J. Liu, *Angew. Chem. Int. Ed.* **2018**, *57*, 8865-8870; d) C. Fang, Y. Huang, L. Yuan, Y. Liu, W. Chen, Y. Huang, K. Chen, J. Han, Q. Liu, Y. Huang, *Angew. Chem. Int. Ed.* **2017**, *56*, 6793-6797; e) Z. Luo, L. Liu, Q. Zhao, F. Li, J. Chen, *Angew. Chem. Int. Ed.* **2017**, *56*, 12561-12565; f) X. Zhou, Q. Liu, C. Jiang, B. Ji, X. Ji, Y. Tang, H. M. Cheng, *Angew. Chem. Int. Ed.* 10.1002/anie.201814294.

[4] a) Y. Liang, Z. Tao, J. Chen, *Adv. Energy Mater.* **2012**, *2*, 742-769; b) H. Banda, D. Damien, K. Nagarajan, A. Raj, M. Hariharan, M. M. Shaijumon, *Adv. Energy Mater.* **2017**, 1701316; c) H. Zhao, J. Wang, Y. Zheng, J. Li, X. Han, G. He, Y. Du, *Angew. Chem. Int. Ed.* **2017**, *56*, 15334-15338; d) H. Wang, S. Yuan, Z. Si, X. Zhang, *Energy Environ. Sci.* **2015**, *8*, 3160-3165.

[5] a) Z. Song, Y. Qian, X. Liu, T. Zhang, Y. Zhu, H. Yu, M. Otani, H. Zhou, *Energy Environ. Sci.* **2014**, *7*, 4077-4086; b) H. Wang, S. Yuan, D. Ma, X. Huang, F. Meng, X. Zhang, *Adv. Energy Mater.* **2014**, *4*, 1301651; c) T. Sun, Z. Li, H. Wang, D. Bao, F. Meng, X. Zhang, *Angew. Chem. Int. Ed.* **2016**, *128*, 10820-10824; d) Z. Song, H. Zhan, Y. Zhou, *Angew. Chem. Int. Ed.* **2010**, *49*, 8444-8448.

[6] a) P. Hu, H. Wang, Y. Yang, J. Yang, J. Lin, L. Guo, *Adv. Mater.* **2016**, *28*, 3486-3492; b) M. Miroshnikov, K. P. Divya, G. Babu, A. Meiyazhagan, L. M. R. Arava, P. M. Ajayan, G. John, *J. Mater. Chem. A* **2016**, *4*, 12370-12386; c) J. Hong, M. Lee, B. Lee, D.-H. Seo, C. B. Park, K. Kang, *Nat. Commun.* **2014**, *5*, 5335.

[7] a) Y. Su, Y. Liu, P. Liu, D. Wu, X. Zhuang, F. Zhang, X. Feng, *Angew. Chem. Int. Ed.* **2014**, *53*, 1812-1816; b) Z. Song, H. Zhou, *Energy Environ. Sci.* **2013**, *6*, 2280-2301; c) K. Sakaushi, G. Nickerl, F. M. Wisser, D. Nishio-Hamane, E. Hosono, H. Zhou, S. Kaskel, J. Eckert, *Angew. Chem. Int. Ed.* **2012**, *51*, 7850-7854; d) Y. Xu, M. Zhou, Y. Lei, *Mater. Today* **2018**, *21*, 60-78; e) L. Zhu, A. Lei, Y. Cao, X. Ai, H. Yang, *Chem. Commun.* **2013**, *49*, 567-569; f) G. Dai, Y. He, Z. Niu, P. He, C. Zhang, Y. Zhao, X. Zhang, H. Zhou, *Angew. Chem. Int. Ed.* 10.1002/anie.201901040.

[8] a) C. Liu, D. Shen, Q. Chen, *J. Am. Chem. Soc.* **2007**, *129*, 5814-5815; b) Y. Yamamoto, A. Yamamoto, S. Furuta, M. Horie, M. Kodama, W. Sato, K. Akiba, S. Tsuzuki, T. Uchimaru, D. Hashizume, F. Iwasaki, *J. Am. Chem. Soc.* **2005**, *127*, 14540-14541.

[9] M. Liao, S. Scheiner, *J. Chem. Phys.* **2002**, *117*, 205-219.

[10] a) J. Y. Shin, T. Yamada, H. Yoshikawa, K. Awaga, H. Shinokubo, *Angew. Chem. Int. Ed.* **2014**, *53*, 3096-3101; b) T. Ma, Z. Pan, L. Miao, C. Chen, M. Han, Z. Shang, J. Chen, *Angew. Chem. Int. Ed.* **2018**, *57*, 3158-3162; c) P. Gao, Z. Chen, Z. Zhao-Karger, J. E. Mueller, C. Jung, S. Klyatskaya, T. Diemant, O. Fuhr, T. Jacob, R. J. Behm, M. Ruben, M. Fichtner, *Angew. Chem. Int. Ed.* **2017**, *56*, 10341-10346; d) F. Xu, H. Xu, X. Chen, D. Wu, Y. Wu, H. Liu, C. Gu, R. Fu, D. Jiang, *Angew. Chem. Int. Ed.* **2015**, *54*, 6814-6818; e) H. Liao, H. Wang, H. Ding, X. Meng, H. Xu, B. Wang, X. Ai, C. Wang, *J. Mater. Chem. A*, **2016**, *4*, 7416-7421.

[11] K. S. Lokesh, A. Adriaens, *Dyes Pigments* **2015**, *112*, 192-200.

[12] a) L. Fan, Q. Liu, Z. Xu, B. Lu, *ACS Energy Lett.* **2017**, *2*, 1614-1620; b) M. L. Aubrey, J. R. Long, *J. Am. Chem. Soc.*, **2015**, *137*, 13594-13602.

[13] a) V. Augustyn, J. Come, M. A. Lowe, J. W. Kim, P. L. Taberna, S. H. Tolbert, H. D. Abruña, P. Simon, B. Dunn, *Nat. Mater.* **2013**, *12*, 518-522; b) C. Chen, Y. Wen, X. Hu, X. Ji, M. Yan, L. Mai, P. Hu, B. Shan, Y. Huang, *Nat. Commun.* **2015**, *6*, 6929; c) H. Wang, Q. Wu, Y. Wang, X. Wang, L. Wu, S. Song, H. Zhang, *Adv. Energy Mater.* **2019**, *9*, 1802993.

[14] a) C. Jiang, Y. Fang, W. Zhang, X. Song, J. Lang, L. Shi, Y. Tang, *Angew. Chem. Int. Ed.* **2018**, *57*, 16370-16374; b) G. Wang, F. Wang, P. Zhang, J. Zhang, T. Zhang, K. Müllen, X. Feng, *Adv. Mater.* **2018**, *30*, 1802949; c) B. Ji, F. Zhang, N. Wu, Y. Tang, *Adv. Energy Mater.* **2017**, *7*, 1700920; d) X. Tong, F. Zhang, B. Ji, M. Sheng, Y. Tang, *Adv. Mater.* **2016**, 28, 9979-9985; e) J. Lang, J. Li, F. Zhang, X. Ding, J. A. Zapien, Y. Tang, *Batteries & Supercaps* 10.1002/batt.201800138.

10.1002/anie.201904242

WILEY-VCH

Entry for the Table of Contents

COMMUNICATION

A bipolar and self-polymerized phthalocyanine complex is used as the polarity-switchable and high-performance electrode material for lithium-based and graphite-based dual ion batteries, even all-organic symmetric dual ion batteries. This work can bridge the gap between organic batteries and dual ion batteries.

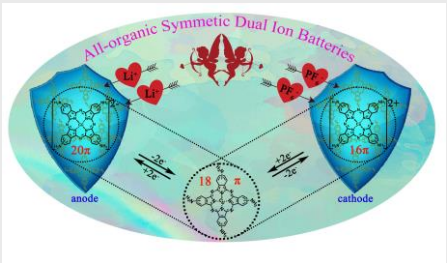

Heng-guo Wang, Haidong Wang, Zhenjun Si, Qiang Li, Qiong Wu, Qi Shao, Lanlan Wu, Yu Liu, Yinghui Wang, Shuyan Song and Hongjie Zhang*

Page No. – Page No.

A bipolar and self-polymerized phthalocyanine complex for fast and tunable energy storage